Quantitative changes in organ-specific amyloid load in a patient with AL amyloidosis, measured by ^{124}I-AT-01 PET/CT imaging, correlate with serum biomarkers

Alan Stuckey[1], Emily Martin[1], R. Eric Heidel[1], Stephen J. Kennel[1], Timothy J. Perk[2], Amy J. Weisman[2], Jonathan Wall[1]

[1]University of Tennessee Graduate School of Medicine, Knoxville TN, 37920, USA. [2]AIQ Solutions, USA

BACKGROUND: The amyloid imaging agent, ^{124}I-AT-01 (aka ^{124}I-p5+14), is being developed for the detection and diagnosis of systemic amyloid deposits, of any type, by PET/CT imaging (1,2). This reagent could provide a facile, first-line method for the diagnosis of amyloidosis as well as permit quantitative longitudinal imaging for monitoring organ-specific progression or regression of disease. In the first-in-human imaging study at the University of Tennessee Medical Center (NCT03678259), one patient with multi-organ AL amyloidosis was imaged twice, 23 months apart, using ^{124}I-AT-01.

OBJECTIVE: Here we report a case study of a patient with AL amyloidosis who had responded positively to anti-plasma cell (daratumumab-based) immunotherapy who underwent repeat PET/CT imaging. The goal was to quantitatively assess changes in amyloid load (based on ^{124}I-AT-01 retention), in the heart, liver, spleen and kidneys assessed from PET/CT images by using both manual (single slice) and automated (fully 3D) methods. These data are evaluated in the context of serum biomarkers of organ function and free light chain levels.

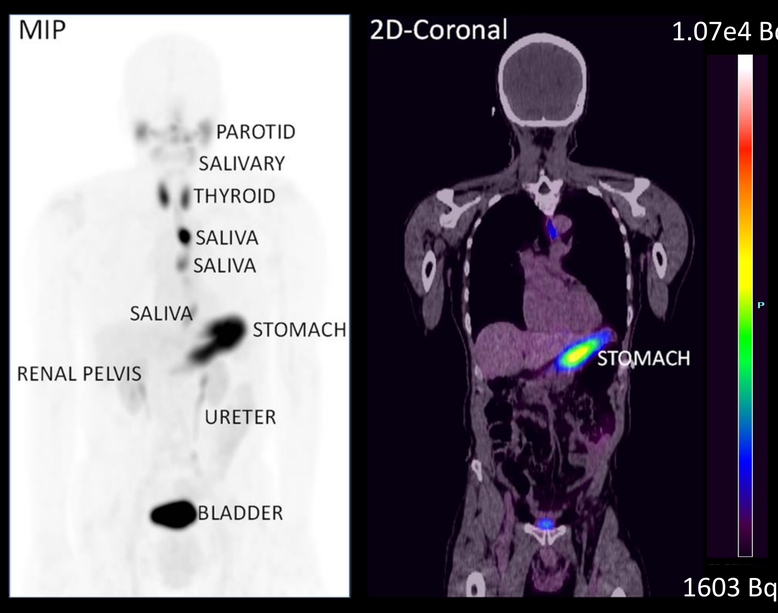

Figure 1. Representative images of ^{124}I-AT-01 in a healthy individual. Maximum intensity projection (left) and 2D coronal PET/CT (right) images reveal physiological distribution of free iodide following dehalogenation of the radiotracer (during renal catabolism), in the parotid, salivary and thyroid glands, the stomach lumen, and areas of renal excretion, including the renal pelvis, ureter and bladder.

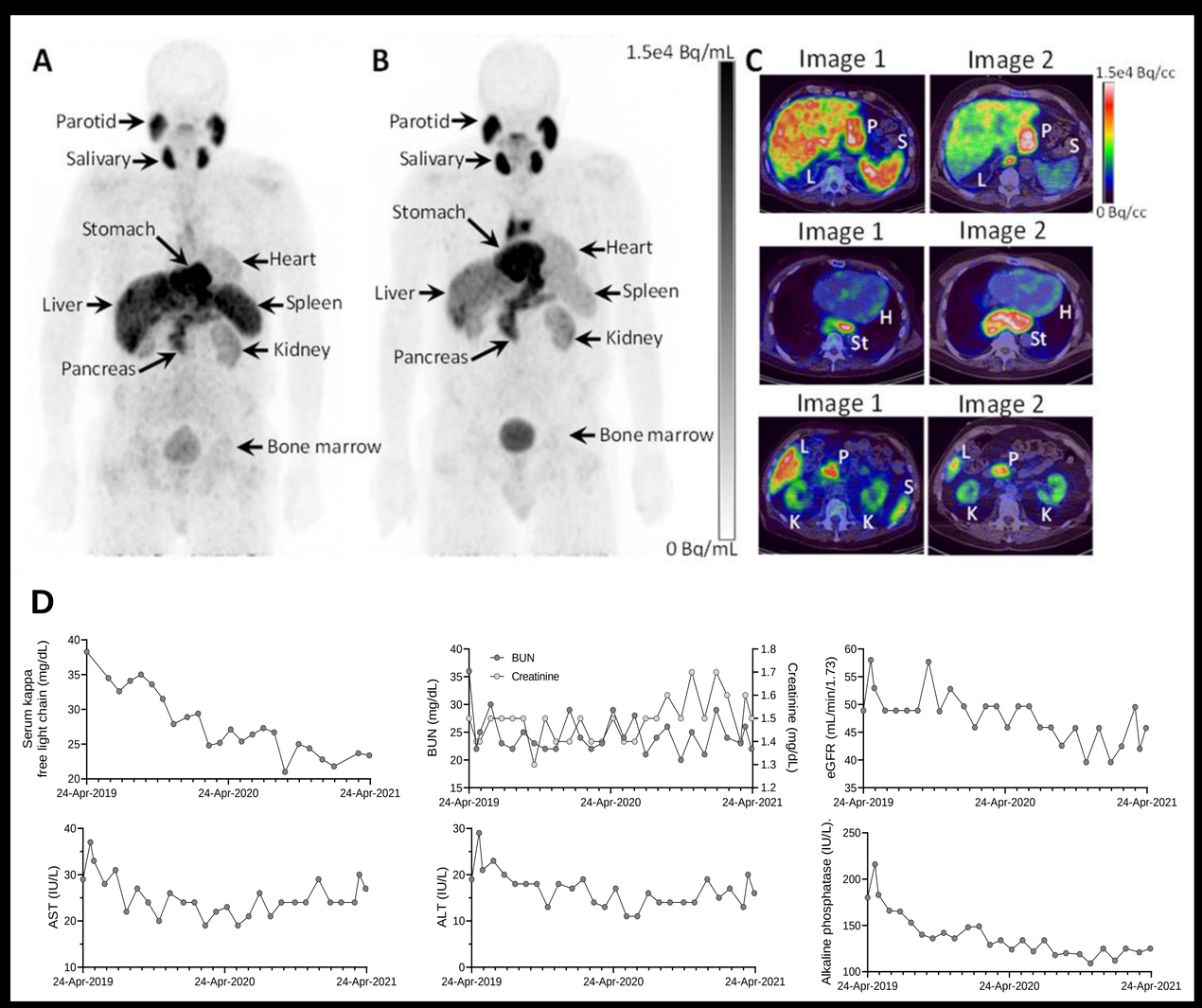

Figure 2. Comparison of ^{124}I-AT-01 images of an AL patient obtained 23 months apart and coincident biomarker trends. Maximum intensity projections from the first (A) and the second (B) scans reveal radiotracer uptake in the heart, liver, spleen, kidneys and pancreas, as well as physiological distribution in the parotids, salivary glands, stomach and bladder. (C) 2D coronal slices of the PET/CT images indicate a decrease of radiotracer uptake in the liver and spleen. (D) Serum biomarker changes over 23 months (L, liver; S, spleen; P, pancreas; H, heart; St, stomach; K, kidney).

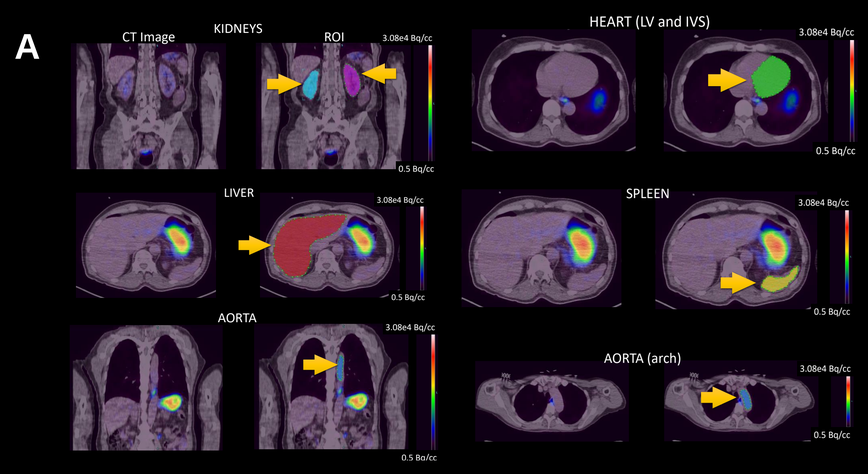

Figure 3. Image analysis using 2D and 3D regions of interest. (A) Single slice ROIs were manually drawn on the PET/CT image for the kidneys, liver, aorta (and aortic arch), heart (LV; left ventricle, IVS; interventricular septum), and spleen, as indicated with yellow arrows.

B

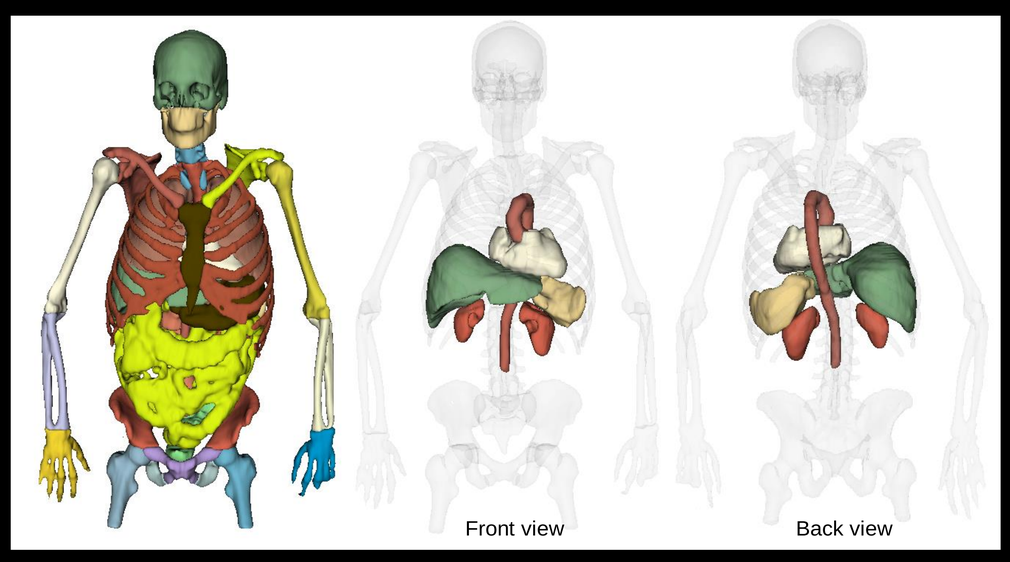

C

2D ANALYSIS	$SUVR_{mean}$ Scan 1	$SUVR_{mean}$ Scan 2	Change (%)
Liver	4.63	3.45	-25.5
Spleen	5.11	2.24	-56.3
Kidneys	2.38	2.68	12.8
Heart	1.62	1.94	19.6

3D ANALYSIS	$SUVR_{mean}$ Scan 1	$SUVR_{mean}$ Scan 2	Change (%)
Liver	3.92	3.03	-22.6
Spleen	3.96	1.85	-53.2
Kidneys	2.21	2.49	13.1
Heart	1.39	1.65	18.2

Figure 3 (B) Fully 3D segmented organs were achieved using TRAQinform IQ technology. (C) Compiled data, expressed as mean SUVR and percent change between the first and second scans, from 2D and 3D ROI analysis reveal similar results with both techniques.

D

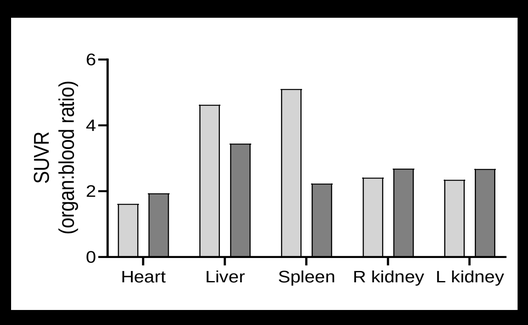

Figure 3 (D) Mean SUVR measurements obtained with manual 2D ROI analysis from the first imaging session (light grey) and the second imaging session (dark grey) show a decrease in ^{124}I-AT-01 uptake in the liver and spleen.

RESULTS: The PET/CT images indicated amyloid uptake of the radiotracer in the heart, spleen, liver, kidneys, pancreas and bone marrow, with physiological distribution of radioactivity in the parotid and salivary glands, stomach lumen and urinary bladder.

In the second scan, hepatosplenic radioactivity had visually decreased relative to heart and kidney. Quantitative analysis of PET/CT images by manual 2D and automated 3D methods correlated significantly ($rP < 0.98$; $p < 0.02$). Changes in hepatic, splenic, renal and cardiac radiotracer uptake were -22.6%, -53.2%. +13.1%, +18.2% for the manual method, and -25.5%, -56.3%, +12.9%, +19.64% for the automated method. Concurrent with the ~24% decrease in hepatic amyloid, serum alkaline phosphatase decreased 40% (~200 IU/mL to ~120 IU/mL), both occurring in the context of a hematologic response and 40% decrease in serum free light chain levels.

SUMMARY: Organ-specific changes in amyloid load can be visualized and quantified using ^{124}I-AT-01. In this patient, changes in the hepatic amyloid load were consistent with improved organ function based on serum alkaline phosphatase measurements. However, reduction in hepatosplenic amyloid may have occurred in the context of stable or slightly increasing amyloid deposition in the heart and kidneys. Serum NTproBNP decreased between imaging sessions from 729 pg/mL to 401 pg/mL.

Organ-specific amyloid regression and progression, and biomarker-based response to therapy following anti-plasma cell therapies, remains a complex phenomenon in patients with systemic AL amyloidosis. PET/CT imaging using ^{124}I-AT-01 may play a valuable role not only in the diagnosis of amyloidosis but also for monitoring changes in organ-specific amyloid load.

This study was supported in part with services from the NHLBI, through the Science Moving TowArds Research Translation and Therapy (SMARTT) program. The authors acknowledge funding support from grant CHE1904577 (RRJ) and contributions to the Amyloidosis and Cancer Theranostics Gift Fund (including CMC/Gerdau, Knoxville)

THE UNIVERSITY of TENNESSEE
GRADUATE SCHOOL OF MEDICINE